Parabrachial nucleus activity in nociception and pain in awake mice

Abbreviated title: Parabrachial nucleus in nociception and pain in awake mice

Jesse Andrew Smith[1], Yadong Ji[2], Rebecca Lorsung[1], Macauley Smith Breault[3], Jeffrey Koenig[4], Nathan Cramer[1], Radi Masri[1,2], Asaf Keller[1]

[1] University of Maryland, Program in Neuroscience, Department of Neurobiology
[2] Department of Advanced Oral Sciences and Therapeutics, University of Maryland School of Dentistry
[3] Picower Institute for Learning and Memory, Massachusetts Institute of Technology, Cambridge, MA, USA
[4] University of Maryland, Program in Molecular Medicine, Department of Neurobiology

The authors declare no competing financial interests.

Correspondence should be addressed to Asaf Keller at akeller@som.umaryland.edu

22 pages; 9 figures, 1 table
Number of words: Abstract - 159; Introduction - 447; Discussion – 953

This work was supported by National Institutes of Health National Institute of Neurological Disorders and Stroke Grants R01NS099245 and R01NS069568. The content is solely the responsibility of the authors and does not necessarily represent the official views of the National Institutes of Health. The funding sources had no role in study design; the collection, analysis and interpretation of data; the writing of the report; or in the decision to submit the article for publication.

Abstract

The parabrachial nuclear complex (PBN) is a nexus for aversion, and for the sensory and affective components of pain perception. We have previously shown that, during chronic pain, PBN neurons in anesthetized rodents have amplified activity. We report a method to record from PBN neurons of behaving, head-restrained mice, while applying reproducible noxious stimuli. We find that both spontaneous and evoked activity are higher in awake animals, compared to urethane anesthetized mice. Fiber photometry of calcium responses from CGRP-expressing PBN neurons demonstrates that these neurons respond to nociceptive stimuli. In both males and females with neuropathic or inflammatory pain, responses of PBN neurons remain amplified for at least 5 weeks, in parallel with increased pain metrics. We also show that PBN neurons can be rapidly conditioned to respond to innocuous stimuli, after pairing with nociceptive stimuli. Finally, we demonstrate that changes in PBN neuronal activity are correlated with changes in arousal, measured as changes in pupil diameter.

Significance Statement

The parabrachial complex is a nexus of aversion, including pain. We report a method to record from parabrachial nucleus neurons of behaving mice, while applying reproducible noxious stimuli. This allowed, for the first time, tracking the activity of these neurons over time in animals with neuropathic or inflammatory pain. It also allowed us to show that the activity of these neurons correlates with arousal states, and that these neurons can be conditioned to respond to innocuous stimuli.

Introduction

Pain is a multidimensional experience, composed of unpleasant sensory, affective and cognitive experiences (Melzack and Casey, 1968; Fields, 1999; Price, 2000; Treede et al., 2000; Auvray et al., 2010). Because of the multidimensionality of the pain experience, chronic pain patients suffer from comorbid emotional and cognitive deficits, and exhibit alterations in the function of brain networks linked to these deficits (Borsook, 2012; Bushnell et al., 2013). Therefore, treating pain, and especially chronic pain, requires addressing not only the sensory aspects of pain, but also its affective and cognitive components.

Chronic pain affecting the trigeminal system, in particular, is associated with deficits in affective processing, including increases in anxiety and depression (Smith et al., 2013; Wu et al., 2015; Turnes et al., 2022). A key region in the trigeminal system is the parabrachial nuclear complex (PBN). It is a nexus of aversion and of both the nociceptive and affective components of pain processing (Chiang et al., 2019). PBN is involved in other aversive behaviors (Cai et al., 2018), including taste aversion (Carter et al., 2015; Chen et al., 2018), threat memory (Han et al., 2015), and fear conditioning (Campos et al., 2018; Bowen et al., 2020). We and others have found that PBN neurons respond to noxious stimuli under urethane anesthesia (Bernard and Besson, 1990; Uddin et al., 2021) and display amplified activity during chronic pain (Uddin et al., 2018; Raver et al., 2020).

Most of what is known about the physiology of PBN in the context of pain comes from studies using anesthetized animals. This is problematic because anesthesia may blunt pain related activity. Further, anesthesia does not allow studies of state-dependent changes in pain perception, changes that are critical to pain behavior. Pain perception depends on both external stimuli and the internal state of the animal. Internal states—such as distraction (Buhle and Wager, 2010; Legrain et al., 2011) or hunger (Alhadeff et al., 2018)—profoundly alter pain perception. Therefore, it is essential to determine how internal states affect PBN processing in behaving animals.

Recordings of nociceptive responses from PBN in awake animals are complicated by at least two major technical difficulties. First, the location of PBN—at the junction of the midbrain and pons and its relation to major vessels—renders recordings from single units unstable and of low signal to noise ratio in behaving animals. The second complication is the ability to present to behaving animals reproducible noxious stimuli. We have adapted a head-restrained, awake rodent recording model to address these issues. This allowed us to investigate the physiology of PBN in awake animals in response to both noxious and non-noxious stimuli and the role of internal states in PBN processing.

Methods

We adhered to accepted standards for rigorous study design and reporting to maximize the reproducibility and translational potential of our findings, as described by Landis et al. (2012) and in ARRIVE (Animal Research: Reporting In Vivo Experiments). In line with National Institutes of Health recommendations for scientific rigor, we performed an a priori power analysis to estimate required sample sizes (Landis et al., 2012).

Animals

All procedures were conducted according to Animal Welfare Act regulations and Public Health Service guidelines and approved by the University of Maryland School of Medicine Animal Care and Use Committee. We used 27 male and female wild type C57BL/6 mice from Jackson Laboratory (JAX strain # 000644): 9 CCI-ION animals, 4 CFA injected animals, and 14 naïve animals. We also used 8 CGRP-CRE mice, 4 male and 4 female, that were bred in house from breeding pairs obtained from Jackson Laboratory (JAX stock # 033168).

Animals were housed in a 12 h dark/light cycle, and food and water were given ad libitum. The animals were group-housed prior to headplate surgery. After surgery they were individually housed.

Headplate Implant Surgery

Animals were induced with 2-4% isoflurane and placed in a stereotaxic frame. The anesthesia was maintained at 1-2% for the surgery. Animals were given Rimadyl (5 mg/kg) for analgesia. The skin on the top of the skull was removed and the headplate (Model 11, Neurotar, Helsinki, Finland) was secured to the skull using a mixture of dental cement and Vetbond (3M, USA). Two screws were implanted anterior to the headplate for grounding. A craniotomy was created to expose the brain above PBN (AP 4.8mm-5.3mm, ML 0.5mm-2mm) and the dura was removed. The area was cleaned using a cortical buffer with antibiotics (125mM NaCl, 5mM KCl, 10mM Glucose, 10mM HEPES, 2mM 1M $CaCl_2$, 2mM 1M $MgCl_2$, 100 units/ml penicillin, 0.1 mg/ml streptomycin). The craniotomy was closed using a silicone elastomer (QuikSil, World Precision Instruments, Sarasota, FL, USA). The animal was placed on a heating pad and allowed to recover.

Training

Animals were trained on the Neurotar Mobile HomeCage (Neurotar) where they were head restrained but allowed to locomote freely on a carbon fiber platform supported by a cushion of air. Animals were given 5 days to recover after the implant of the headplate. On day 6 animals were left in their home cage and placed near the Neurotar setup to habituate to the noise of the air flow for 2 hours. On day 7, animals were placed in the Neurotar setup and allowed to move freely for up to 2 hours to habituate to the device. Electrophysiology recordings started on day 8.

Electrophysiology Recordings

Awake Electrophysiology Recordings

We performed recordings in low light conditions. Animals were placed in the Neurotar setup and allowed to acclimate for 5 minutes. The silicone elastomer was removed and

146 the craniotomy was cleaned using a cortical buffer with antibiotics. A single
147 platinum-iridium recording electrode (0.3-1 MΩ), produced in our lab, was lowered into
148 PBN. We digitized recorded waveforms using a Plexon system (Plexon Inc., Dallas,
149 TX). We isolated units that were responsive to noxious heat (50ºC) applied to the
150 anterior maxillary region of the head using a Picasso Lite dental surgical laser (AMD
151 Lasers, Indianapolis, IN), positioned 5 mm above the skin, set to 3.5 W for 5 seconds.
152 The laser was calibrated with a Jenco Electronics microcomputer thermometer to
153 generate 51°C at the end of a 5 second exposure. We waited at least 2 minutes
154 between consecutive stimuli and inspected the skin after each stimulus for erythema or
155 tissue damage. Upon finding a neuron that was responsive to noxious heat stimulation,
156 we allowed the cell to return to its baseline firing rate before recording baseline
157 spontaneous activity for 5 minutes. After that, we recorded responses to noxious heat
158 applied at 2 minute intervals to prevent tissue damage for a total of 10-12 trials. After
159 each recording session, the electrode was removed and the craniotomy was cleaned
160 using a cortical buffer with antibiotics and covered with fresh silicone elastomer.

161 *Anesthetized Electrophysiology Recordings*

162 Animals were anesthetized via intraperitoneal injections of urethane (10% w/v).
163 Following anesthesia, the mice were placed in a stereotaxic frame with a heating pad
164 and a craniotomy was made over the recording site to target PBN (AP 4.8mm-5.3mm,
165 ML 0.5mm-2mm). The recording and stimulation protocol was identical to the awake
166 mice protocol.

167 *Electrophysiology Data Analysis*

168 Recordings were sorted using Offline Sorter (Plexon Inc., Dallas, TX) using dual
169 thresholds and principal component analysis. Responses to thermal stimuli were
170 analyzed with custom MATLAB scripts. Significant responses were defined as firing
171 activity exceeding the 95% confidence interval of the average pre-stimulus firing rate.
172 Thus, evoked responses are expressed as significant responses above baseline firing
173 levels. Peristimulus time histograms (PSTHs) were generated to analyze responses to
174 repeated stimuli.

175 We defined after-discharges—periods of sustained activity that outlast a stimulus
176 presentation (Okubo et al., 2013)—as PSTH bins in which activity exceeded the 95%
177 confidence interval for a period lasting at least 5 seconds after stimulus offset.

178 **CCI-ION**

179 We used a rodent model of neuropathic pain that was induced by chronic constriction of
180 the infraorbital nerve (CCI-ION) (Bennett and Xie, 1988; Uddin et al., 2018; Raver et al.,
181 2020). Animals were anesthetized with ketamine/xylazine (100/10 mg/kg, i.p.). We
182 made intraoral incisions along the roof of the mouth, beginning distal to the first molar.
183 The ION was freed from the surrounding connective tissue and loosely tied with a silk
184 thread (4-0) 1-2 mm from the nerves emerging from the infraorbital foramen. Animals
185 were monitored for 2 days in their home cage as they recovered. Each animal served as
186 its own control, as recordings were compared before and after CCI in each animal.

187 **CFA**

188 We used complete Freund's adjuvant (CFA) to induce persistent inflammatory pain.

Animals were induced with 2-4% isoflurane and injected with 15 µL of CFA (Sigma-Aldrich F5881. Sigma, St. Louis, MO, USA) subcutaneously in the snout, ipsilateral to the recording site. Animals were monitored for 24 hours in their home cage as they recovered before recording. Each animal served as its own control, as above.

Behavior

Facial Grimace

To assess ongoing pain, we analyzed facial grimace behaviors in animals placed in the Neurotar Mobile HomeCage and images of the face were taken every 60 seconds for 15 minutes. Animals were scored with defined action units (AU) that examined orbital tightening, nose bulging, whisker positioning, and cheek bulging to derive a mouse grimace score (MGS) (Langford et al., 2010; Akintola et al., 2017). We calculated MGS as the average score of all the AUs.

Mechanical Sensitivity

To assess mechanical sensitivity, animals were placed in the Neurotar Mobile HomeCage and von Frey filaments (North Coast Medical) were applied to the anterior maxillary region, ipsilateral to CCI or CFA injections. A response was defined by an active swipe of the filament with the forepaws. We used the up-down method to determine response thresholds, as described previously (Dixon, 1965; Chaplan et al., 1994; Akintola et al., 2017; Raver et al., 2020). For each mouse, baseline response thresholds were determined prior to CCI-ION/CFA injections and thresholds were reassessed on each day of recordings from PBN. Hyperalgesia was defined as mechanical withdrawal threshold ≥ 20% below baseline.

Viral Construct Injection

We anesthetized the animals with isoflurane and placed them in a stereotaxic frame. Either left or right PBN (-5.2mm AP, ±1.5mm ML, -2.2 to -2.9mm DV) was targeted via a small craniotomy. We injected 0.5 µL of AAV9-syn.Flex.GCaMP6f.WPRE. SV40 (Addgene #100833) at a rate of 0.1 µL/min using glass pipettes (40-60 µm tip diameter), coupled to a Hamilton syringe controlled by a motorized pump. The pipette was left in place for 10 minutes before being slowly retracted over 5-10 min. Headplates were implanted immediately after the virus injections.

Because AAV9 can be transported retrogradely (Castle et al., 2014), recorded signals might reflect activity in axons projecting to PBN. We carefully considered this possibility by analyzing histological sections through structures that project to PBN. We did not detect retrogradely labeled cells in any of these structures.

Fiber Photometry

Recording

We anesthetized animals using 2% isoflurane and placed them in a stereotaxic frame. Mice were implanted with a fiber optic probe (400 µM diameter, 0.39NA; RWD Life Sciences) in the PBN (-5.2mm AP, +1.5mm ML, -2.2 to -2.5mm DV) during the same surgery they were injected with the viral construct and the head plate was implanted. The mice were given 3 weeks to recover and to allow for viral expression in their home cage.

231 For recordings, the fiber optic probe was connected to an RZX10 LUX fiber photometry
232 processor running Synapse software (Tucker-Davis Technologies) through a Doric mini
233 cube (Doric Lenses). LEDs at 465 nm and 405 nm were used for GCaMP excitation and
234 isosbestic control, respectively. LED power was calibrated weekly using a digital optical
235 power meter (Thor Labs).

236 *Analysis*

237 We used pMat (Bruno et al., 2021) to quantify photometry signals as changes in
238 GCaMP fluorescence. These were converted to Z-Scores that were time-locked using a
239 time window starting 5 seconds before the onset of the noxious stimulus and lasting
240 until 30 seconds post-stimulus for each trial. A significant response was defined as one
241 exceeding the 95% confidence interval of the baseline across all trials. The duration and
242 AUC were calculated using the significant response of the Z-Score averaged across
243 trials.

244 **Conditioning**

245 *Recordings*

246 Mice were head restrained in the Neurotar Mobile Homecage and recordings were
247 determined to be responsive to noxious heat (see above). While recording pupil size
248 (see below) and firing rate of PBN neurons, we presented the mouse with a tone (1
249 second, 100 kHz, 88 dB) 10 times with 2 minutes intervals. We administered a
250 conditioning paradigm where a 1 second tone (CS) was paired with a 5 second noxious
251 heat stimulus (US), where the tone was presented 3 seconds after the onset of the
252 noxious heat, to align with the laser reaching noxious temperature. This pairing was
253 repeated 15 times at 1 minute intervals. The CS was presented until extinction with 2
254 minute between presentations of the CS. We then administered the conditioning
255 paradigm a second time. The CS was again presented until extinction.

256 The firing rates of conditioned trials were binned at 0.1 seconds before being split into
257 trials time-locked at the stimuli onset. A significant response was defined as exceeding
258 the 95% confidence interval of the baseline across all trials.

259 *Pupillometry*

260 We videotaped pupils in head restrained mice, under low light conditions using a
261 webcam (Logitech Brio, Logitech Inc., Newark, CA). Recordings were acquired at 30 Hz
262 using custom MATLAB® scripts and the Image Acquisition Toolbox (Mathworks, Natick,
263 MA). Noxious heat stimulation timestamps were recorded by a microcontroller (Arduino
264 Uno R3, 2015) using a custom script in Python (Python Software Foundation,
265 https://www.python.org/). These timestamps aligned the video with the
266 electrophysiological data. Pupil area was measured from the videos offline using
267 Facemap software (Stringer et al., 2019). We excluded times when Facemap detected
268 that the animal blinked. Pupil area was normalized between [0,1] using the minimum
269 and maximum value within each recording session. Normalized pupil areas of
270 conditioned trials were binned at 0.1 seconds before being split into trials time-locked at
271 the stimuli onset. A significant response was defined as exceeding the 95% confidence
272 interval of the baseline across all trials.

273 We defined spontaneous activity as activity at least 3 minutes before the onset of the

first stimulus. Firing rates and normalized pupil areas during this time were binned using a width of 1 second. The normalized pupil areas were down-sampled to accommodate the bins of the spike rate by calculating the median within each bin. We applied a minimum cut-off of 10 Hz to the firing rates. To investigate the relationship between spontaneous activity and normalized pupil area we quantified it as the Pearson correlation coefficient.

To determine the relative time dynamics between firing rates and normalized pupil area after heat stimuli trials, we calculated a cross-correlation to produce lag values. This was done by binning the firing rates and normalized pupil areas using a width of 0.1 seconds and splitting them into trials, time-locked around the stimulus onsets. The lag that maximized the magnitude of correlation was selected for further analysis. The firing rates and normalized pupil area used for cross-correlation were then shifted using this lag before taking the Pearson correlation coefficient.

Statistical analysis

We analyzed group data using GraphPad Prism version 9 for Mac (GraphPad Software, La Jolla CA) and custom scripts in MATLAB. Unless otherwise noted, data are presented as median ± 95% confidence intervals (95% CI). Unless otherwise indicated we used nonparametric Mann-Whitney *U* tests because data were not normally distributed. Individual statistical tests were run for each animal, as shown in the figures. We then averaged data from all animals for each condition to calculate group comparisons, and Cohen's *d* was calculated for effect size. Correlations are Pearson correlations.

Results

Anesthesia suppresses spontaneous and evoked PBN responses

PBN neurons recorded in anesthetized animals respond robustly to nociceptive inputs (Bernard and Besson, 1990; Uddin et al., 2018; Raver et al., 2020; Uddin et al., 2021). We developed an approach to apply reproducible noxious stimuli to awake, head-restrained mice, while recording well-isolated single units from the PBN nuclear complex (PBN; Figs. 1, 2). Nociceptive stimuli were generated by a laser-generated light spot (3mm diameter) applied to the snout. This generated a heat stimulus that increased—during the 5 second stimulus period—from body temperature to 50°C (red bar in Fig. 1A, B). Figure 1 compares examples of peri-event histograms recorded from individual PBN neurons in an anesthetized mouse (Fig. 1A) and in an awake mouse (Fig. 1B). In the neuron from the awake animal, spontaneous activity, shown before the onset of the noxious heat, is markedly higher than that in the anesthetized animals. The amplitude of the response is also larger in the neuron from the awake animal.

Group data comparisons quantify the differences in response properties in anesthetized and awake mice (Fig. 1C-E). Spontaneous firing rates were, on average, more than 5 times higher in awake mice (Fig. 1C, Cohen's d 1.09, $p < 10^{-4}$, Table 1). As detailed in Methods, we considered significant responses spiking activity that exceeded the 95th percent confidence interval of the average pre-stimulus firing rate. We computed response magnitude and duration of these significant response epochs. Response magnitudes (computed as spikes per stimulus per bin) were, on average more than 5 times higher in awake mice (Fig. 1D, Cohen's d 1.49, $p = 0.003$, Table 1), compared to those in anesthetized mice. Response durations were similar in neurons from awake and anesthetized mice (Fig. 1E, $p > 0.99$, Table 1).

PB^{CGRP} neurons are activated in response to acute pain

PBN neurons that respond to nociceptive stimuli, and whose activity is related to chronic pain conditions, are in the lateral portion of the PBN (Uddin et al., 2018; Raver et al., 2020). Many neurons in this region express calcitonin gene-related peptide (CGRP), a peptide implicated in aversive behaviors, including pain (Campos et al., 2018; Palmiter, 2018; Chiang et al., 2020). To test if PBN neurons that express CGRP (PB^{CGRP} neurons) respond to noxious stimuli, we used in vivo calcium imaging with fiber photometry to record population activity of PB^{CGRP} neurons.

Figures 3A-C depict GCaMP expression in PB^{CGRP} neurons of a male (B) and female (C) mouse, and the location of the optical fiber (A). An example of a heat-evoked CGaMP response is shown in Figure 3D. The portions of the response that exceeds the 95% confidence interval above the mean baseline levels, indicated by the dotted horizontal line, was defined as significant and labeled in green. The color bar shows the increase in heat, from room temperature to 50°C, which is just above the heat pain threshold for these animals. This threshold was determined based on published data, and on the known activation threshold of relevant nociceptors (Yeomans and Proudfit, 1996; Deuis et al., 2017).

We averaged responses recorded over 4 days from each animal. The duration and area under the curve (AUC) of these responses, from 8 animals (4 of each sex), are depicted

339 in Figure 3E (data from the animal shown in Fig. 3D are marked in green circles in Fig.
340 3E). This experiment was not powered to test for sex differences. These findings
341 demonstrate that PB^{CGRP} neurons respond robustly to noxious heat stimuli applied to
342 the trigeminal region.

343 **Neuropathic pain is associated with hyperactivity of PBN neurons in awake**
344 **animals**

345 We, and others, have shown—in anesthetized rodents—that the activity of PBN
346 neurons is amplified in models of chronic pain (Matsumoto et al., 1996; Uddin et al.,
347 2018; Raver et al., 2020). We tested whether similar changes occur also in awake
348 animals. As in our previous studies (Uddin et al., 2018; Raver et al., 2020), we used the
349 chronic constriction injury of the infraorbital nerve (CCI) model, developed by Bennet
350 and Xie (1988), to induce persistent pain-like behaviors. We tested mechanical
351 hypersensitivity of the face in head restrained mice using a modified version of the
352 "up-down method" (Chaplan et al., 1994) (see Methods). In each of the four animals
353 with CCI, mechanical withdrawal thresholds were lower than in pre-CCI levels (Fig. 4A),
354 indicating that the mice experienced increased tactile hypersensitivity. These changes
355 were recorded between 8 and 56 days after CCI surgery.

356 We used mechanical hypersensitivity as a behavioral readout because the thermal
357 hypersensitivity tests of the face were unreliable, as even 0.1 W power differences in
358 the calibrated laser output—the finest differences in power output the laser could
359 produce—resulted in fluctuating behavioral responses. This may be due to the high
360 sensitivity of the face to the thermal stimulation. Mechanical sensitivity tests, on the
361 other hand, produced consistent behavioral responses at each filament level.

362 To assess ongoing pain, we used the mouse grimace scale (MGS) (Langford et al.,
363 2010; Akintola et al., 2017). MGS scores were higher in mice after CCI, relative to
364 controls, and remained higher for as long as they were recorded (up to 8 weeks) (Fig.
365 4B), suggesting that CCI mice were exhibiting persistent, ongoing pain.

366 We compared recordings of well isolated, single units from PBN in the same mice
367 before and after CCI. There were distinct changes in the response magnitude and
368 duration, but not the spontaneous activity, of PBN neurons after CCI (Fig. 4 E-G).
369 Figure 4 shows an example of peri-event rasters and peri-event histograms recorded
370 from individual PBN neurons in the same animal before (Fig. 4C) and 7 days after CCI
371 (Fig. 4D). The neuron recorded after CCI showed an increase in both the magnitude
372 and the duration of responses to heat stimuli applied to the face. In this neuron,
373 spontaneous activity is also higher after CCI, however, when averaged across animals,
374 spontaneous activity did not change after CCI (see below). The neurons recorded
375 before CCI began responding at approximately 45ºC, presumably the nociceptive
376 threshold. In contrast, the neuron recorded after CCI began to fire at temperatures well
377 below noxious threshold, at approximately 30ºC (Fig. 4C and D). Before CCI, all
378 neurons from all animals responded only to nociceptive temperatures; after CCI, all
379 neurons also responded to innocuous temperatures.

380 We quantified the differences in response properties before and after CCI for each of
381 the mice (Fig. 4E-G). We included, as post-CCI data, neurons recorded from two to
382 eight weeks after CCI, a period in which all animals displayed tactile hypersensitivity

383 and increased MGS scores. There was no difference in spontaneous firing rates after
384 CCI in any of the animals (Fig. 4E), but there was an increase in the magnitude of the
385 response (Fig. 4G, Table 1) and response duration (Fig. 4F, Table 1). The magnitude of
386 the responses was 3 times larger after CCI (Fig. 4G, effect size 0.5, $p < 10^{-4}$) and
387 response durations were 3.25 times longer (Fig. 4F, effect size 0.5, $p < 10^{-4}$). Median
388 response duration after CCI was 10.5 seconds, far outlasting the duration of the
389 stimulus. These prolonged responses are defined as after-discharges (Matsumoto et al.,
390 1996; Uddin et al., 2018; Raver et al., 2020). The increase in response duration is
391 consistent with our previous findings, in anesthetized rodents, demonstrating that
392 chronic pain is associated with an increase in the incidence and duration of
393 after-discharges in PBN neurons (Uddin et al., 2018; Raver et al., 2020).

394 We investigated sex differences by pooling 90 neurons recorded from 8 animals (4 of
395 each sex). In naïve animals, there were no sex differences in spontaneous activity (p =
396 0.4, median (males)= 24.65, CI (males) = 20.51,42.72; median (females) = 29.95, CI
397 (females) = 24.38,38.66), response duration (p = 0.84, median (males) = 4.8, CI (males)
398 = 7.767, 20.94; median (females) = 5.3, CI (females) = 7.971, 17.63) or response
399 magnitude (p = 0.9, median (males) = 37.95, CI (males) = 53.29, 166.6; median
400 (females) = 35.05, CI (females) = 41.97, 76.39). Similarly, there were no sex differences
401 after CCI in spontaneous activity (p = 0.34, median (males) = 32.45, CI (males) = 28.57,
402 77.52; median (females) = 25.9, CI (females) = 22.15, 62.45), response duration (p =
403 0.97, median (males) = 10.2, CI (males) = 10.09, 15.25; median (females) = 10.85, CI
404 (females) = 9.53, 19.89), or response magnitude (p = 0.07, median (males) = 371.5, CI
405 (males) = 292, 564.8; median (females) = 154, CI (females) = 108.5, 422.4).

406 **Time-course of changes in PBN activity**

407 By recording from awake animals, we were able to investigate the time course of the
408 activity of PBN neurons before and after the induction of nerve injury, and to determine
409 the relationship between the activity of PBN neurons and the pain behaviors in
410 individual animals. Figure 5 plots the duration (Fig. 5A) and magnitude (Fig. 5B) of
411 responses in each of the neurons, pooled from the 4 animals, across time. Response
412 duration and magnitude remained elevated relative to pre-CCI levels for at least 5
413 weeks post-CCI period, a period in which the animals experienced hyperalgesia (Fig.
414 5A). We recorded a small number of neurons from animals 6 to 8 weeks post-CCI;
415 although some of these neurons had elevated activity (Fig. 5A, B), the small sample
416 size precludes conclusions about activity levels at these time points.

417 **Anesthesia suppresses the effects of CCI on PBN activity**

418 We showed, above, that anesthesia suppresses the responses of PBN neurons to acute
419 nociceptive inputs (Fig. 1). We also showed that CCI results in amplification of PBN
420 responses, recorded from awake rodents (Fig. 4). Here, we tested if this amplification
421 was affected by anesthesia. That is, we directly compared PBN activity after CCI, in
422 anesthetized vs awake mice.

423 Group data comparisons quantified the differences in responses to noxious heat stimuli
424 in anesthetized and awake mice after CCI (Fig. 6). Spontaneous firing rates were more
425 than 3 times higher in awake mice (Fig. 6A, effect size 4.5, p = 0.03). Response
426 magnitudes were more than 5 times higher in awake mice (Fig. 6C, effect size 5.5, p =

427 0.003). Response durations were similar in neurons from awake and anesthetized mice
428 (Fig. 6B; $p > 0.99$). These findings indicate that spontaneous activity and responses to
429 nociceptive stimuli in PBN neurons of CCI mice are larger in the awake, compared to
430 anesthetized animals, but that the duration of after-discharges is similar in these
431 conditions.

432 **Inflammatory pain is associated with hyperactivity of PBN neurons in awake**
433 **animals**

434 To determine if similar changes in PBN activity occur also in other models of pain, we
435 induced, in a separate group of animals, inflammatory pain by injection of complete
436 Freund's adjuvant (CFA) in the snout. We assessed tactile hypersensitivity levels at the
437 snout daily on each of the 3 days before CFA injections, and on days 2 to 6 after
438 injections. After CFA, mechanical thresholds decreased (Fig. 7A) indicating that the
439 mice were experiencing increased tactile hypersensitivity.

440 Between 2 and 6 days after CFA application, there were changes in the spontaneous
441 and evoked activity of PBN neurons. Figure 7 depicts an example of peri-event rasters
442 and peri-event histograms recorded from individual PBN neurons in the same animal
443 before (Fig. 7B) and after CFA (Fig. 7C). After CFA, there were increases in
444 spontaneous activity, response duration, and response magnitude in all animals tested
445 (Fig.7D-F).

446 We quantified the differences in response properties before and 6 days after CFA in
447 each of the awake mice (Fig. 7D-F). Unlike in CCI animals, there was an increase in
448 spontaneous firing rates after CFA (Table 1). Neurons from all animals were pooled into
449 pre and post CFA groups, revealing an average 3.3-fold increase in spontaneous
450 activity (Fig. 7D, effect size 0.49, $p < 10^{-4}$). The increase in spontaneous activity may
451 reflect the persistent inflammatory nature of CFA pain, which may not be as prominent
452 in animals with CCI. Just as with the CCI animals, response durations were 2.7 times
453 longer (Fig. 7E, effect size 0.49, $p < 10^{-4}$) and response magnitudes were 2.7 times
454 larger after CFA (Fig. 7F, effect size 0.52, $p < 10^{-4}$) in all animals tested, indicating the
455 presence of amplified after discharges. Taken together with the CCI data, these data
456 indicate that mouse models of both neuropathic pain (CCI) and inflammatory pain (CFA)
457 are associated with hyperactivity of PBN neurons in awake mice.

458 We investigated sex differences by pooling 42 neurons recorded all 4 animals (2 males
459 and 2 females). In animals recorded after CFA injections, there were no differences in
460 spontaneous activity ($p = 0.59$, median (males) = 51.7, CI (males) = 43.94, 100.7;
461 median (females) = 61.9, CI (females) = 51.64, 98.86), response duration ($p = 0.13$,
462 median (males) = 12.3, CI (males) = 10.54, 16.21; median (females) = 10.7, CI
463 (females) = 10.04, 11.94), or response magnitude ($p = 0.92$, median (males) = 432.4, CI
464 (males) = 307.8, 662.3; median (females) = 340, 566.9).

465 **PBN activity is correlated with arousal**

466 A benefit of recording from awake animals is the ability to test the hypothesis that PBN
467 activity can be modulated by the “behavioral state” of an animal. One approach to
468 assess behavioral states is to measure pupil size as a proxy of the arousal state (de
469 Gee et al., 2020).

Spontaneous activity rates were correlated with pupil area. Figure 8A depicts a representative recording session, plotting changes in both pupil area (blue) and the spontaneous firing rate of a PBN neuron (red). Note that pupil dilations appear to immediately precede increases in the neuronal firing rate. Figure 8B quantifies this relationship by plotting instantaneous neuronal firing rates (1 second bins) against pupil are, demonstrating a positive correlation between these metrics. A significant, positive correlation was seen in 14 out of 17 cells across all 7 animals tested (4 males, 3 females), with r values ranging from 0.55 to 0.12. These findings suggest that arousal states—approximated by changes in pupil diameter—correlate with changes in PBN activity.

To determine if arousal states affect evoked responses of PBN neurons, we constructed and overlayed PSTHs (0.1 second bin size) of neuronal activity and pupil area (Fig. 8C). The PSTHs were aligned to the onset of the 5 second heat stimuli applied to the snout. Pupil dilation and PBN activity after the onset of the noxious heat were highly correlated (Fig. 8C,D, $r = 0.83$, $p = 1.75 \times 10^{-13}$). A significant positive correlation was seen in 13 neurons from 7 animals tested, with r values ranging from 0.9 to 0.5. Four cells had a negative correlation (Fig. 8D). Cross correlation analysis revealed that, in the majority of cells recorded (15 of 17) there was a positive lag, indicating that changes in PBN activity preceded changes in pupil area (Fig. 8E).

Auditory conditioning of PBN activity

Pairing activation of PBN neurons with sucrose produces robust and long-lasting conditioned taste aversion in mice, whereas suppressing PBN activity suppresses the acquisition and expression of this conditioned aversion (Carter et al., 2015; Chen et al., 2018). These findings suggest that the activity of PBN neurons can be conditioned to respond to innocuous stimuli. To test this, we conditioned head-restrained mice by pairing an auditory tone (1 second, 100 kHz, 80 dB) with a noxious heat stimulus applied to the snout. We did this while recording from nociceptive neurons in the PBN nucleus. Figure 9 depicts an example of one of these recording sessions.

Before conditioning, the PBN neuron responded to the heat stimulus (not shown), but not to the auditory stimulus (Fig. 9A). We used 15 pairings of auditory tone (1 second) and heat (5 seconds) stimuli, with the auditory stimulus presented 3 seconds after the onset of the noxious heat stimulus, so that the auditory stimulus is presented just before the heat reaches noxious temperatures. After the pairing session, the neuron responded robustly to the auditory tone, and continued to do so for a median of 13 presentations of the tone (delivered every 120 seconds; Fig. 9A, range = 16-10 stimuli). After the tone responses extinguished, we delivered a second session of 15 pairings of the auditory tone and heat stimuli, after which the neuron again began responding to the auditory stimulus, and did so for the next 14 stimuli, until this auditory response extinguished (Fig. 9B, median = 13.5 stimuli, range = 20-9 stimuli). Sham pairings (see methods; “unconditioned tone”), where the auditory tone was presented without the noxious heat stimulus, had no effect on PBN activity (Fig. 9, grey traces).

We conditioned nociceptive PBN neurons to auditory stimuli in 24 neurons from 7 animals (4 males, 3 females), using the conditioning paradigm described above while measuring pupil size changes. None of these neurons responded to auditory stimuli

514 before conditioning, but all of them began responding to the auditory stimuli after
515 conditioning. Significant responses to auditory stimuli could be evoked for 6 to 22 stimuli
516 (median =13) after the conditioning. All the neurons could be conditioned again after
517 extinction of the auditory stimuli. Pupil size significantly increased after the conditioning
518 paradigm in 10 out of the 14 neurons recorded (Fig 9C,D). These data suggest that
519 PBN neurons that respond to noxious heat stimuli can be conditioned to respond to an
520 innocuous auditory tone.

521 **Discussion**

522 **Anesthesia alters properties of PBN neurons**

523 Much of what we know about the neurophysiology of nociception and pain originates
524 from studies using anesthetics which may alter neuronal responses to noxious stimuli.
525 Some anesthetics nearly completely suppress responses of PBN neurons (Luo et al.,
526 2018; Melonakos et al., 2021). We and others have found that PBN neurons do respond
527 to noxious stimuli under urethane anesthesia (Bernard and Besson, 1990; Uddin et al.,
528 2018; Raver et al., 2020; Uddin et al., 2021). Here we show that those responses are
529 different from the ones recorded in awake animals. In awake animals, spontaneous
530 PBN neuronal activity is, on average, 3 times higher and PBN responses to noxious
531 stimuli are, on average, 5 times larger in amplitude than those in urethane anesthetized
532 animals. In contrast, response duration was indistinguishable in awake and
533 anesthetized animals.

534 **PB^{CGRP} neurons respond to noxious stimuli**

535 PBN neurons expressing calcitonin gene-related peptide (CGRP) have been implicated
536 in driving pain behaviors. Inhibition of PB^{CGRP} neurons attenuates pain behaviors (Han
537 et al., 2015). PB^{CGRP} neurons are also involved in acute pain perception, as they
538 respond to acute noxious stimuli (Campos et al., 2018; Kang et al., 2022). Our findings
539 corroborate this conclusion, demonstrating that populations of PB^{CGRP} neurons respond
540 robustly to thermal noxious stimuli.

541 One study reported that CGRP application in PBN can produce analgesia, and that this
542 effect is blocked by sub-nanomolar concentrations of a CGRP antagonist (Wang et al.,
543 2021). To our knowledge, this is the only report suggesting that CGRP might be
544 anti-nociceptive. In contrast, we and others have found that PB^{CGRP} neurons robustly
545 increase their activity in response to nociceptive stimuli.

546 **PBN activity correlates with internal states**

547 Recordings from awake animals are required to determine how “internal states” might
548 affect PBN activity and pain perception. Internal states directed towards distractions,
549 such as cognitively demanding tasks, can affect pain perception. Detection of a noxious
550 stimulus is compromised while performing a working memory-intensive task (Buhle and
551 Wager, 2010). Inflammatory pain is attenuated in states of hunger, through a process
552 involving neuropeptide Y (NPY) signaling (Alhadeff et al., 2018); manipulating NPY in
553 PBN can mimic hunger states, suggesting a role of PBN in this state-dependent pain
554 modulation. Similarly, suppressing PBN activity inhibits arousal (Kaur et al., 2017),
555 whereas activating PBN neurons increases arousal (Kaur and Saper, 2019).

556 We found a direct correlation between PBN activity and arousal, as measured by pupil
557 size, during presentation of a noxious stimulus. Since changes in PBN activity preceded
558 changes in pupil size, PBN activity may be influencing internal states. A potential
559 concern is that thermal stimulation may directly lead to pupil dilation, independent of
560 central mechanisms. This is because thermal stimulation of the snout activates the V1
561 branch of the trigeminal nerve (Kim et al., 2014), potentially causing pupil dilation via the
562 ciliary nerve, which contains fibers from the V1 branch of the trigeminal nerve (Joo et
563 al., 2014; McDougal and Gamlin, 2015). However, our finding that pupil size and PBN

activity are correlated in the absence of heat stimuli argues against this possibility.

Nociceptive PBN neurons can be conditioned to respond to an auditory tone

In addition to its role in nociception and arousal, the PBN is also involved in aversive behaviors. For example, stimulating the PBN induces conditioned taste aversion, whereas silencing it attenuates conditioned taste aversion (Carter et al., 2015; Chen et al., 2018). Optogenetic stimulation of the PBN nucleus induces context-dependent freezing, demonstrating its involvement with threat memory and fear conditioning (Han et al., 2015; Campos et al., 2018; Bowen et al., 2020). Although these studies show that PBN neurons are necessary and sufficient for fear conditioning, they do not elucidate the underlying function of specific PBN neurons. We found that the same PBN neurons that respond to noxious stimuli can be conditioned to respond to non-noxious stimuli. Changes in pupil size mirrored this conditioned behavior. These findings suggest that conditioned aversion may involve plasticity in the response properties of PBN neurons, consistent with evidence for a causal role of the PBN in conditioned aversive behaviors (Carter et al., 2015; Campos et al., 2018; Chen et al., 2018; Bowen et al., 2020).

The auditory-nociceptive conditioning paradigm in our study evoked short-lasting conditioning of both pupil dilation responses and PBN responses to the conditioned auditory stimuli (Fig. 9). In contrast, conditioned aversion induced by pairing direct stimulation of the PBN with tastants, or pairing tastants with appetite-suppressing substances, produced aversive behaviors that can last days (Carter et al., 2015; Campos et al., 2018; Chen et al., 2018; Bowen et al., 2020). A causal role for the PBN in this long-lasting aversion is supported by finding that suppressing PBN activity attenuates the conditioned behavior (Carter et al., 2015; Campos et al., 2018; Chen et al., 2018; Bowen et al., 2020).

Our findings (Fig. 9) confirm that individual PBN neurons can respond to multiple modalities (Sammons et al., 2016; Campos et al., 2018; Bowen et al., 2020), including to nociceptive stimuli (Kang et al., 2022). Individual PBN neurons can respond during the conditioning phase, where a noxious stimulus is paired with a non-noxious tone, but they do not respond when presented with the conditioned tone 24 hours later (Kang et al., 2022). Our findings show that the same PBN neurons that respond to noxious heat can be rapidly conditioned to respond to an auditory tone, confirming that PBN neurons may be responsible for aversive memory formation. However, we also show that this conditioned response is short lived, lasting only up to one hour after conditioning, suggesting that PBN neurons may be involved in short term aversive memory retrieval but not in long term aversive memory retrieval.

Figure Legends

Figure 1: PBN neurons in anesthetized mice respond substantially differently than in awake animals.

A: PSTHs recorded from PBN neurons in a urethane-anesthetized and awake (B) mice. Color bar indicates application of heat from a laser, producing temperatures that peak at 50°C. Note different y-axes scales. C: Spontaneous firing rates and magnitude of responses to noxious heat applied to the face (D) were higher in awake mice (Mann-Whitney U = 109.5, p < 10-4 and U = 13, p < 10-4). E: Response durations were indistinguishable in awake and anesthetized mice. Data are medians and 95% confidence intervals.

Figure 2: Recordings sites in PBN.

Locations of recording sites, derived from stereotaxic coordinates, indicated by red markers (for neurons recorded from awake animals) or blue markers (for neurons recorded from anesthetized animals). Numbers indicate the number of recordings from the same location. Kölliker-fuse nucleus (KF), lateral PBN (LPB), dorsal part of the lateral PBN nucleus (LPBD), central part of the lateral PBN nucleus (LPBC), external part of the lateral PBN nucleus (LPBE), internal part of the lateral PBN nucleus (LPBI), superior part of the lateral PBN nucleus (LPBS), ventral part of the lateral PBN nucleus (LPBV), medial PBN nucleus (MPB), external part of the medial PBN nucleus (MPBE), superior cerebellar peduncle (scp). Image maps from Paxinos & Franklin, 2019.

Figure 3: PB^{CGRP} neurons respond to noxious stimuli.

GCaMP expression in PB^{CGRP} neurons of a male (B) and female (C) mouse, and the location of the optical fiber (A). D: Heat-evoked GCaMP response, with significant portion of the response—exceeding the 95% confidence interval above the baseline levels—indicated by dotted horizontal line and labeled in green. Color bar shows the increase in heat, from room temperature to 50°C. E: Response duration and area under the curve (AUC) of these responses, from 8 animals (4 of each sex). Data from the animal shown in D are marked in green circles.

Figure 4: Neuropathic pain is associated with hyperactivity of PBN neurons in awake animals.

Time course of reductions in facial tactile hypersensitivity (A) and increases in mouse grimace scores (B) in each of the four mice (M=male; F=female), after CCI. Representative raster plots and PSTHs of neurons recorded from the same animal before (C) and after (D) CCI, in response to noxious heat applied to the snout. Color bar shows the increase in heat from room temperature to 50ºC. In each of the mice spontaneous activity was not affected after CCI (E), whereas response durations (F) and magnitudes (G) increased. Data represent medians and 95% confidence intervals; p-values derived from Mann-Whitney tests.

641

642 **Figure 5**: Time course of changes in PBN activity after CCI.

643 Response durations (A) and magnitudes (B) remain elevated for at least 5 weeks post
644 CCI (B). Purple markers indicate neurons recorded while animals displayed tactile
645 hyperalgesia. Individual data represent individual neurons, and black bars depict weekly
646 median values.

647

648 **Figure 6**: PBN neurons after CCI are different in awake animals.

649 A: Post-CCI spontaneous firing rates recorded from awake mice were higher than in
650 anesthetized mice. B: There was no difference in response duration in response to
651 noxious heat applied to the face. C: Response magnitude was higher in awake mice
652 than in anesthetized mice in response to noxious heat applied to the face. Markers
653 represent cells (n = 10 cells for anesthetized and 44 for awake). Data represent
654 medians and 95% confidence intervals.

655

656 **Figure 7**: Inflammatory pain is associated with hyperactivity of PBN neurons in awake
657 animals.

658 A: Time course of reductions in facial tactile hypersensitivity in each of the four mice
659 (M=male; F=female), after CFA injection. Representative rasters and PSTHs computed
660 for neurons recorded from the same animal before (B) and after (C) CFA injection, in
661 response to noxious heat applied to the snout for 5 seconds. The color bar shows the
662 increase in heat from room temperature to 50ºC. D: Spontaneous firing rates increased
663 in 3 out of the 4 animals after CFA injections. Both response duration (E) and
664 magnitude (F) increased after CFA in each of the animals. Data represent medians and
665 95% confidence intervals.

666

667 **Figure 8**: PBN activity is correlated with arousal states.

668 A: Representative traces depicting spontaneous firing rates (red) of PBN neurons and
669 normalized pupil area (blue). B: These metrics were positively correlated. C: Averaged
670 (and 95% CI) traces of firing rate of PBN neurons (red) and pupil area (blue) in
671 response to noxious heat applied to the snout. D: The lag-shifted correlation values
672 suggest that firing rate and pupil area changes are positively correlated (n = 17 cells, 7
673 animals). E: The positive lag value after cross-correlation suggests that changes in
674 firing rate preceded changes in pupil area (n = 17 cells, 7 animals).

675

676 **Figure 9**: Innocuous auditory conditioning of PBN responses.

677 A: A noxious heat-responsive PBN neuron does not respond to an innocuous tone
678 before conditioning (black trace) but responds robustly to the tone after a conditioning
679 (red). B: Representative traces showing the same PBN neuron undergoing extinction
680 (black), and responses after a second conditioning paradigm (red). C: Similarly, pupil

681 responses to the innocuous auditory stimulus appear only after the conditioning
682 paradigm (blue). D: Recordings from the same neuron after extinction of the
683 conditioned responses (black trace) and after reconditioning the auditory response
684 (blue). Data represent averages and 95% confidence intervals, indicated by the
685 horizontal dotted lines.

686

687

688

689 **References**

690 Akintola T, Raver C, Studlack P, Uddin O, Masri R, Keller A (2017) The grimace scale
691 reliably assesses chronic pain in a rodent model of trigeminal neuropathic pain.
692 Neurobiol Pain, 2:13–17.

693 Alhadeff AL, Su Z, Hernandez E, Klima ML, Phillips SZ, Holland RA, Guo C, Hantman
694 AW, De Jonghe BC, Betley JN (2018) A Neural Circuit for the Suppression of Pain by a
695 Competing Need State. Cell, 173:140–152.e15.

696 Auvray M, Myin E, Spence C (2010) The sensory-discriminative and
697 affective-motivational aspects of pain. Neurosci Biobehav Rev, 34:214–223.

698 Bennett GJ, Xie YK (1988) A peripheral mononeuropathy in rat that produces disorders
699 of pain sensation like those seen in man. Pain, 33:87–107.

700 Bernard JF, Besson JM (1990) The spino(trigemino)pontoamygdaloid pathway:
701 electrophysiological evidence for an involvement in pain processes. J Neurophysiol,
702 63:473–490.

703 Borsook D (2012) Neurological diseases and pain. Brain, 135:320–344.

704 Bowen AJ, Chen JY, Huang YW, Baertsch NA, Park S, Palmiter RD (2020) Dissociable
705 control of unconditioned responses and associative fear learning by parabrachial CGRP
706 neurons. Elife, 9:e59799.

707 Bruno CA, O'Brien C, Bryant S, Mejaes JI, Estrin DJ, Pizzano C, Barker DJ (2021)
708 pMAT: An open-source software suite for the analysis of fiber photometry data.
709 Pharmacol Biochem Behav, 201:173093.

710 Buhle J, Wager TD (2010) Performance-dependent inhibition of pain by an executive
711 working memory task. Pain, 149:19–26.

712 Bushnell MC, Ceko M, Low LA (2013) Cognitive and emotional control of pain and its
713 disruption in chronic pain. Nat Rev Neurosci, 14:502–511.

714 Cai YQ, Wang W, Paulucci-Holthauzen A, Pan ZZ (2018) Brain circuits mediating
715 opposing effects on emotion and pain. J Neurosci, 38:6340–6349.

716 Campos CA, Bowen AJ, Roman CW, Palmiter RD (2018) Encoding of danger by
717 parabrachial CGRP neurons. Nature, 555:617–622.

718 Carter ME, Han S, Palmiter RD (2015) Parabrachial calcitonin gene-related peptide
719 neurons mediate conditioned taste aversion. J Neurosci, 35:4582–4586.

720 Castle MJ, Gershenson ZT, Giles AR, Holzbaur EL, Wolfe JH (2014) Adeno-associated
721 virus serotypes 1, 8, and 9 share conserved mechanisms for anterograde and
722 retrograde axonal transport. Hum Gene Ther, 25:705–720.

723 Chaplan SR, Bach FW, Pogrel JW, Chung JM, Yaksh TL (1994) Quantitative
724 assessment of tactile allodynia in the rat paw. J Neurosci Methods, 53:55–63.

725 Chen JY, Campos CA, Jarvie BC, Palmiter RD (2018) Parabrachial CGRP Neurons
726 Establish and Sustain Aversive Taste Memories. Neuron, 100:891–899.e5.

727 Chiang MC, Bowen A, Schier LA, Tupone D, Uddin O, Heinricher MM (2019)
728 Parabrachial Complex: A Hub for Pain and Aversion. J Neurosci, 39:8225–8230.

729 Chiang MC, Nguyen EK, Canto-Bustos M, Papale AE, Oswald AM, Ross SE (2020)
730 Divergent Neural Pathways Emanating from the Lateral Parabrachial Nucleus Mediate
731 Distinct Components of the Pain Response. Neuron, 106:927–939.e5.

732 de Gee JW, Tsetsos K, Schwabe L, Urai AE, McCormick D, McGinley MJ, Donner TH
733 (2020) Pupil-linked phasic arousal predicts a reduction of choice bias across species
734 and decision domains. Elife, 9:e54014.

735 Deuis JR, Dvorakova LS, Vetter I (2017) Methods used to evaluate pain behaviors in
736 rodents. Front Mol Neurosci, 10:284.

737 Dixon WJ (1965) The up-and-down method for small samples. Journal of the American
738 Statistical Association, 60:967–978.

739 Fields HL (1999) Pain: an unpleasant topic. Pain, Suppl 6:S61–S69.

740 Han S, Soleiman MT, Soden ME, Zweifel LS, Palmiter RD (2015) Elucidating an
741 Affective Pain Circuit that Creates a Threat Memory. Cell, 162:363–374.

742 Joo W, Yoshioka F, Funaki T, Mizokami K, Rhoton AL (2014) Microsurgical anatomy of
743 the trigeminal nerve. Clin Anat, 27:61–88.

744 Kang SJ, Liu S, Ye M, Kim DI, Pao GM, Copits BA, Roberts BZ, Lee KF, Bruchas MR,
745 Han S (2022) A central alarm system that gates multi-sensory innate threat cues to the
746 amygdala. Cell Rep, 40:111222.

747 Kaur S, Saper CB (2019) Neural Circuitry Underlying Waking Up to Hypercapnia. Front
748 Neurosci, 13:401.

749 Kaur S, Wang JL, Ferrari L, Thankachan S, Kroeger D, Venner A, Lazarus M, Wellman
750 A, Arrigoni E, Fuller PM, Saper CB (2017) A Genetically Defined Circuit for Arousal from
751 Sleep during Hypercapnia. Neuron, 96:1153–1167.e5.

752 Kim YS, Chu Y, Han L, Li M, Li Z, Lavinka PC, Sun S, Tang Z, Park K, Caterina MJ,
753 Ren K, Dubner R, Wei F, Dong X (2014) Central terminal sensitization of trpv1 by
754 descending serotonergic facilitation modulates chronic pain. Neuron,

755 Langford DJ, Bailey AL, Chanda ML, Clarke SE, Drummond TE, Echols S, Glick S,
756 Ingrao J, Klassen-Ross T, Lacroix-Fralish ML, Matsumiya L, Sorge RE, Sotocinal SG,
757 Tabaka JM, Wong D, van den Maagdenberg AM, Ferrari MD, Craig KD, Mogil JS (2010)
758 Coding of facial expressions of pain in the laboratory mouse. Nat Methods, 7:447–449.

759 Legrain V, Crombez G, Mouraux A (2011) Controlling attention to nociceptive stimuli
760 with working memory. PLoS One, 6:e20926.

761 Luo T, Yu S, Cai S, Zhang Y, Jiao Y, Yu T, Yu W (2018) Parabrachial Neurons Promote
762 Behavior and Electroencephalographic Arousal From General Anesthesia. Front Mol
763 Neurosci, 11:420.

764 Matsumoto N, Bester H, Menendez L, Besson JM, Bernard JF (1996) Changes in the
765 responsiveness of parabrachial neurons in the arthritic rat: an electrophysiological
766 study. J Neurophysiol, 76:4113–4126.

767 McDougal DH, Gamlin PD (2015) Autonomic control of the eye. Compr Physiol,
768 5:439–473.

769 Melonakos ED, Siegmann MJ, Rey C, O'Brien C, Nikolaeva KK, Solt K, Nehs CJ (2021)
770 Excitation of Putative Glutamatergic Neurons in the Rat Parabrachial Nucleus Region
771 Reduces Delta Power during Dexmedetomidine but not Ketamine Anesthesia.
772 Anesthesiology, 135:633–648.

773 Melzack R, Casey KL (1968) Sensory, motivational and central control determinants of
774 pain. In: The Skin Senses (Kenshalo DR, ed), pp 423–439. Springfield: Thomas.

775 Okubo M, Castro A, Guo W, Zou S, Ren K, Wei F, Keller A, Dubner R (2013) Transition
776 to persistent orofacial pain after nerve injury involves supraspinal serotonin
777 mechanisms. J Neurosci, 33:5152–5161.

778 Palmiter RD (2018) The Parabrachial Nucleus: CGRP Neurons Function as a General
779 Alarm. Trends Neurosci, 41:280–293.

780 Price DD (2000) Psychological and neural mechanisms of the affective dimension of
781 pain. Science, 288:1769–1772.

782 Raver C, Uddin O, Ji Y, Li Y, Cramer N, Jenne C, Morales M, Masri R, Keller A (2020)
783 An Amygdalo-Parabrachial Pathway Regulates Pain Perception and Chronic Pain. J
784 Neurosci, 40:3424–3442.

785 Sammons JD, Weiss MS, Victor JD, Di Lorenzo PM (2016) Taste coding of complex
786 naturalistic taste stimuli and traditional taste stimuli in the parabrachial pons of the
787 awake, freely licking rat. J Neurophysiol, 116:171–182.

788 Smith JG, Elias LA, Yilmaz Z, Barker S, Shah K, Shah S, Renton T (2013) The
789 psychosocial and affective burden of posttraumatic neuropathy following injuries to the
790 trigeminal nerve. J Orofac Pain, 27:293–303.

791 Stringer C, Pachitariu M, Steinmetz N, Reddy CB, Carandini M, Harris KD (2019)
792 Spontaneous behaviors drive multidimensional, brainwide activity. Science, 364:255.

793 Treede RD, Apkarian AV, Bromm B, Greenspan JD, Lenz FA (2000) Cortical
794 representation of pain: functional characterization of nociceptive areas near the lateral
795 sulcus. Pain, 87:113–119.

796 Turnes JM, Araya EI, Barroso AR, Baggio DF, Koren LO, Zanoveli JM, Chichorro JG
797 (2022) Blockade of kappa opioid receptors reduces mechanical hyperalgesia and
798 anxiety-like behavior in a rat model of trigeminal neuropathic pain. Behav Brain Res,
799 417:113595.

800 Uddin O, Anderson M, Smith J, Masri R, Keller A (2021) Parabrachial complex
801 processes dura inputs through a direct trigeminal ganglion-to-parabrachial connection.
802 Neurobiol Pain, 9:100060.

803 Uddin O, Studlack P, Akintola T, Raver C, Castro A, Masri R, Keller A (2018) Amplified
804 parabrachial nucleus activity in a rat model of trigeminal neuropathic pain. Neurobiol
805 Pain, 3:22–30.

806 Wang LL, Wang HB, Fu FH, Yu LC (2021) Role of calcitonin gene-related peptide in
807 pain regulation in the parabrachial nucleus of naive rats and rats with neuropathic pain.
808 Toxicol Appl Pharmacol, 414:115428.

809 Wu TH, Hu LY, Lu T, Chen PM, Chen HJ, Shen CC, Wen CH (2015) Risk of psychiatric
810 disorders following trigeminal neuralgia: a nationwide population-based retrospective
811 cohort study. J Headache Pain, 16:64.

812 Yeomans DC, Proudfit HK (1996) Nociceptive responses to high and low rates of
813 noxious cutaneous heating are mediated by different nociceptors in the rat:
814 electrophysiological evidence. Pain, 68:141–150.

815

Table I

Figure	Animal	Metric	Comparison	Test Statistic	Median	Sample Size	P value
1C	N/A	Spontaneous activity	Anesthetized vs awake	Mann-Whitney U = 109.5	Anesthetized= 7.94 Awake= 32.80	Anesthetized= 23 cells Awake= 39 cells	$<10^{-4}$
1D	N/A	Response Magnitude	Anesthetized vs awake	Mann-Whitney U = 13	Anesthetized= 10.15 Awake= 44.35	Anesthetized= 23 cells Awake= 28 cells	$<10^{-4}$
1E	N/A	Response Duration	Anesthetized vs awake	Mann-Whitney U = 112	Anesthetized= 4.20 Awake= 4.25	Anesthetized= 8 cells Awake= 28 cells	>0.99
4E	F6	Spontaneous activity	Pre vs Post CCI	Mann-Whitney U = 18	Pre= 20.50 Post= 32.80	Pre= 8 cells Post= 7 cells	0.28
	M9			Mann-Whitney U = 14	Pre= 7.47 Post= 23.25	Pre= 11 cells Post= 6 cells	0.058

	F7			Mann-Whitney U = 41	Pre= 35.35 Post= 25.15	Pre= 8 cells Post= 12 cells	0.624
	M12			Mann-Whitney U = 56	Pre= 43.90 Post= 35.00	Pre= 8 cells Post= 12 cells	0.691
4F	F6	Response Duration	Pre vs Post CCI	Mann-Whitney U = 3.5	Pre= 3.20 Post= 9.40	Pre= 6 cells Post= 7 cells	0.009
	M9			Mann-Whitney U = 0	Pre= 4.25 Post= 9.50	Pre= 6 cells Post= 5 cells	0.0016
	F7			Mann-Whitney U = 3	Pre= 4.40 Post= 11.90	Pre= 8 cells Post= 11 cells	0.0002
	M12			Mann-Whitney U = 0	Pre= 4.70 Post= 10.70	Pre= 7 cells Post= 18 cells	$<10^{-4}$
4G	F6	Response Magnitude	Pre vs Post CCI	Mann-Whitney U = 4	Pre= 24.62 Post= 50.35	Pre= 6 cells Post= 7 cells	0.1143
	M9			Mann-Whitney U = 12	Pre= 23.70 Post= 98.65	Pre= 6 cells Post= 5 cells	0.0353

	F7			Mann-Whitney U = 17	Pre= 58.90 Post=307.00	Pre= 8 cells Post= 11 cells	0.0125
	M12			Mann-Whitney U = 2	Pre= 64.60 Post= 374	Pre= 7 cells Post= 18 cells	$<10^{-4}$
6C	N/A	Spontaneous activity	Anesthetized vs awake Post CCI	Mann-Whitney U = 69.50	Anesthetized= 11.76 Awake= 32.80	Anesthetized= 10 cells Awake= 39 cells	0.0012
6D	N/A	Response Duration	Anesthetized vs awake Post CCI	Mann-Whitney U = 115.5	Anesthetized= 16.70 Awake= 11.15	Anesthetized= 10 cells Awake= 38 cells	0.0586
6E	N/A	Response Magnitude	Anesthetized vs awake Post CCI	Mann-Whitney U = 85	Anesthetized= 65.70 Awake= 282.00	Anesthetized= 10 cells Awake= 41 cells	0.0034
7D	M10	Spontaneous activity	Pre vs Post CFA	Mann-Whitney U = 1	Pre= 2.95 Post= 46.70	Pre= 5 cells Post= 7 cells	0.0051
	F14			Mann-Whitney U = 25	Pre= 29.80 Post= 70.20	Pre= 15 cells Post= 12 cells	0.0009

	F15			Mann-Whitney U = 34	Pre= 28.05 Post= 46.70	Pre= 14 cells Post= 10 cells	0.0358
	M16			Mann-Whitney U = 14	Pre= 26.00 Post= 52.00	Pre= 8 cells Post= 13 cells	0.0045
7E	M10	Response Duration	Pre vs Post CFA	Mann-Whitney U = 0	Pre= 3.50 Post= 12.50	Pre= 5 cells Post= 7 cells	0.0043
	F14			Mann-Whitney U = 3	Pre= 3.90 Post= 9.10	Pre= 16 cells Post= 12 cells	$<10^{-4}$
	F15			Mann-Whitney U = 2	Pre= 2.10 Post=9.18	Pre= 15 cells Post= 10 cells	$<10^{-4}$
	M16			Mann-Whitney U = 0	Pre= 3.78 Post= 9.60	Pre= 8 cells Post= 13 cells	$<10^{-4}$
7F	M10	Response Magnitude	Pre vs Post CFA	Mann-Whitney U = 0	Pre= 11.92 Post=136.00	Pre= 5 cells Post= 7 cells	0.0025
	F14			Mann-Whitney U = 2	Pre= 17.20 Post=354.30	Pre= 13 cells Post= 12 cells	$<10^{-4}$

	F15			Mann-Whitney U = 0	Pre= 36.60 Post=317.50	Pre= 11 cells Post= 8 cells	$<10^{-4}$
	M16			Mann-Whitney U = 1	Pre= 67.60 Post=701.50	Pre= 7 cells Post= 10 cells	0.0002
8B	N/A	N/A	Firing rate vs Pupil size correlation	Spearman's r =0.542	N/A	N/A	$2.36e^{-24}$

Table 1: Statistics for Figures 1 through 9 showing the corresponding figure number, animals, metric, comparisons being made, test statistic, medians or means, sample size, and *p* values.

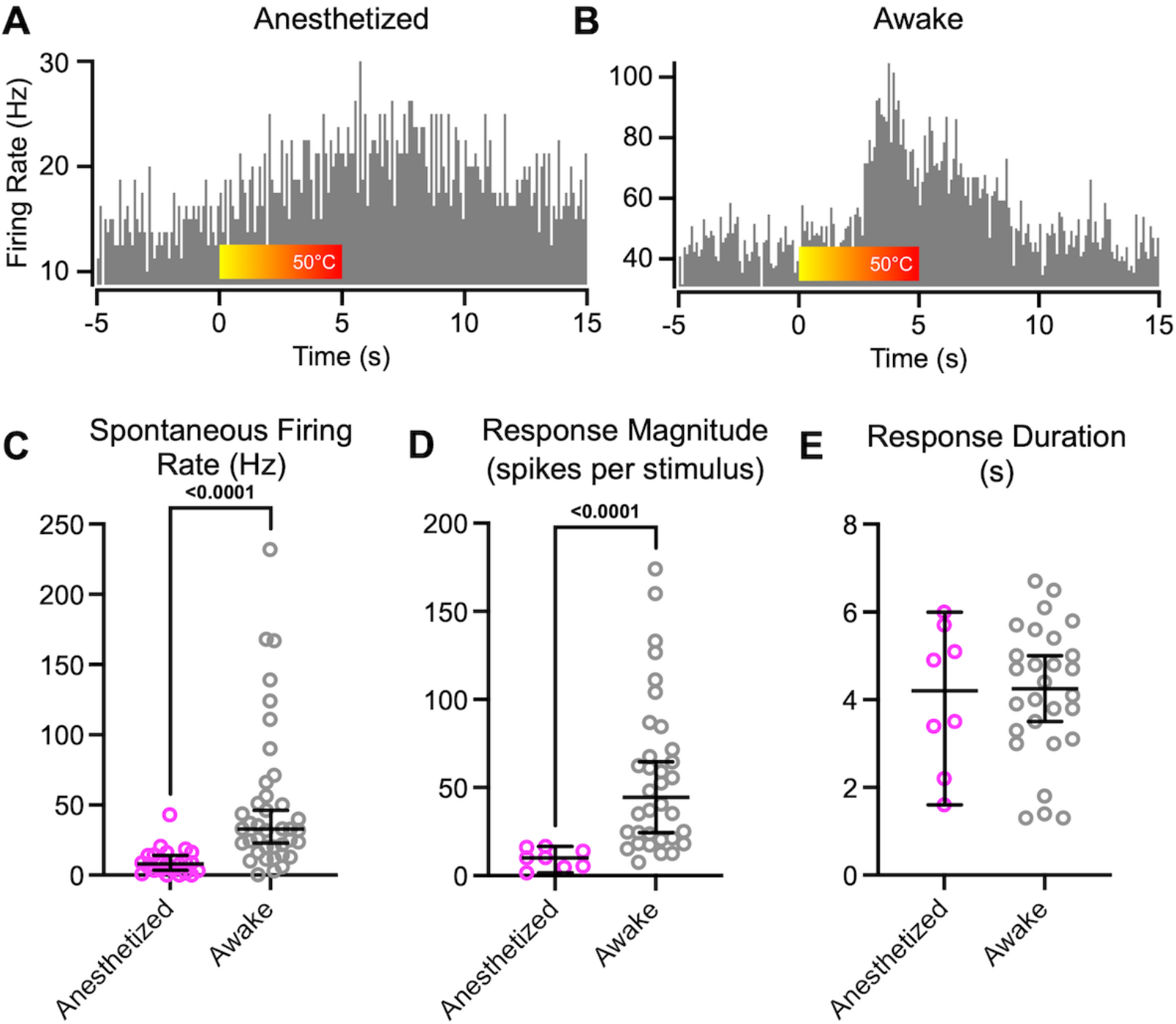
A
Anesthetized
Firing Rate (Hz)
30
20
10
50°C
-5
0
5
10
15
Time (s)
B
Awake
100
80
60
40
50°C
-5
0
5
10
15
Time (s)
C
Spontaneous Firing Rate (Hz)
<0.0001
250
200
150
100
50
0
Anesthetized
Awake
D
Response Magnitude (spikes per stimulus)
<0.0001
200
150
100
50
0
Anesthetized
Awake
E
Response Duration (s)
8
6
4
2
0
Anesthetized
Awake

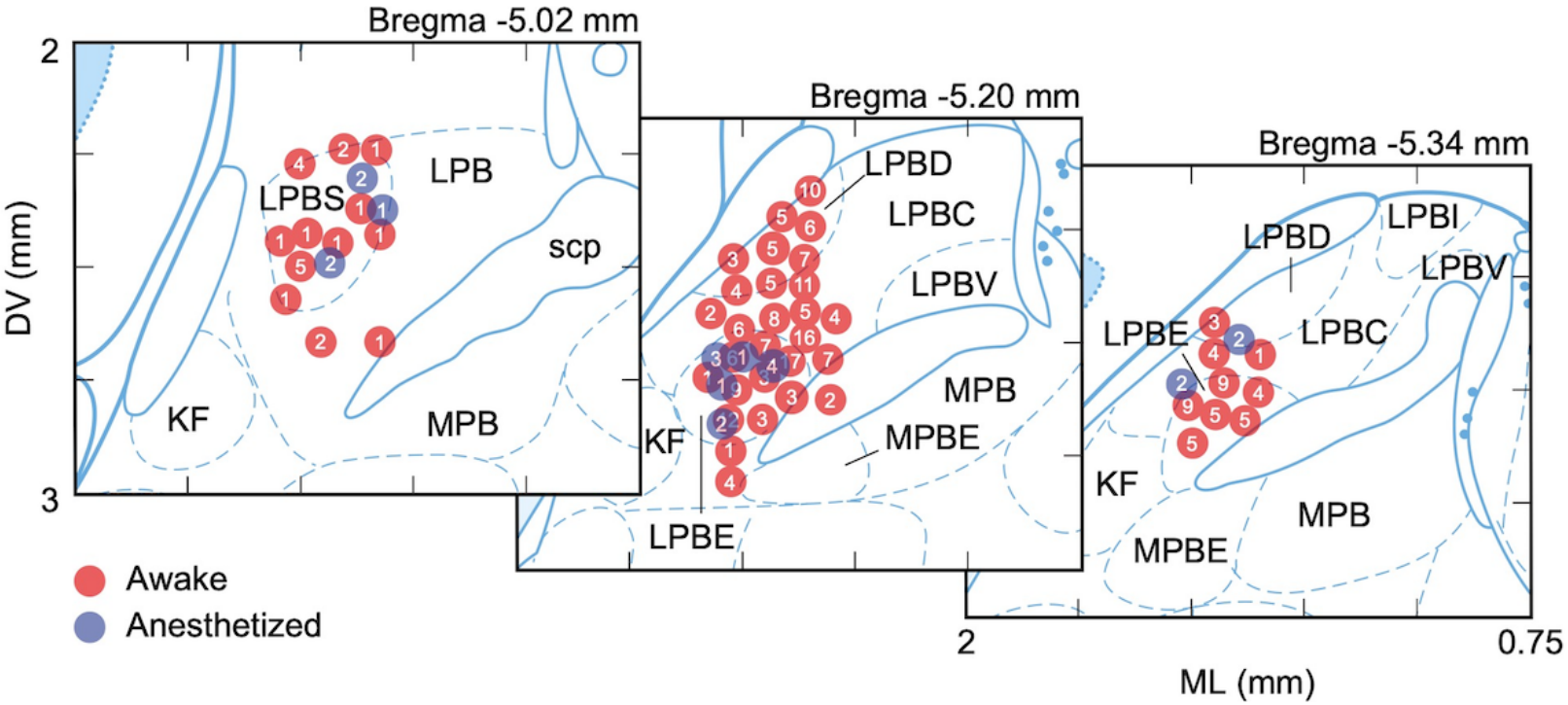
Bregma -5.02 mm
Bregma -5.20 mm
Bregma -5.34 mm
DV (mm)
2
3
ML (mm)
2
0.75
LPB
LPBS
scp
KF
MPB
LPBD
LPBC
LPBV
MPBE
LPBE
LPBI
Awake
Anesthetized

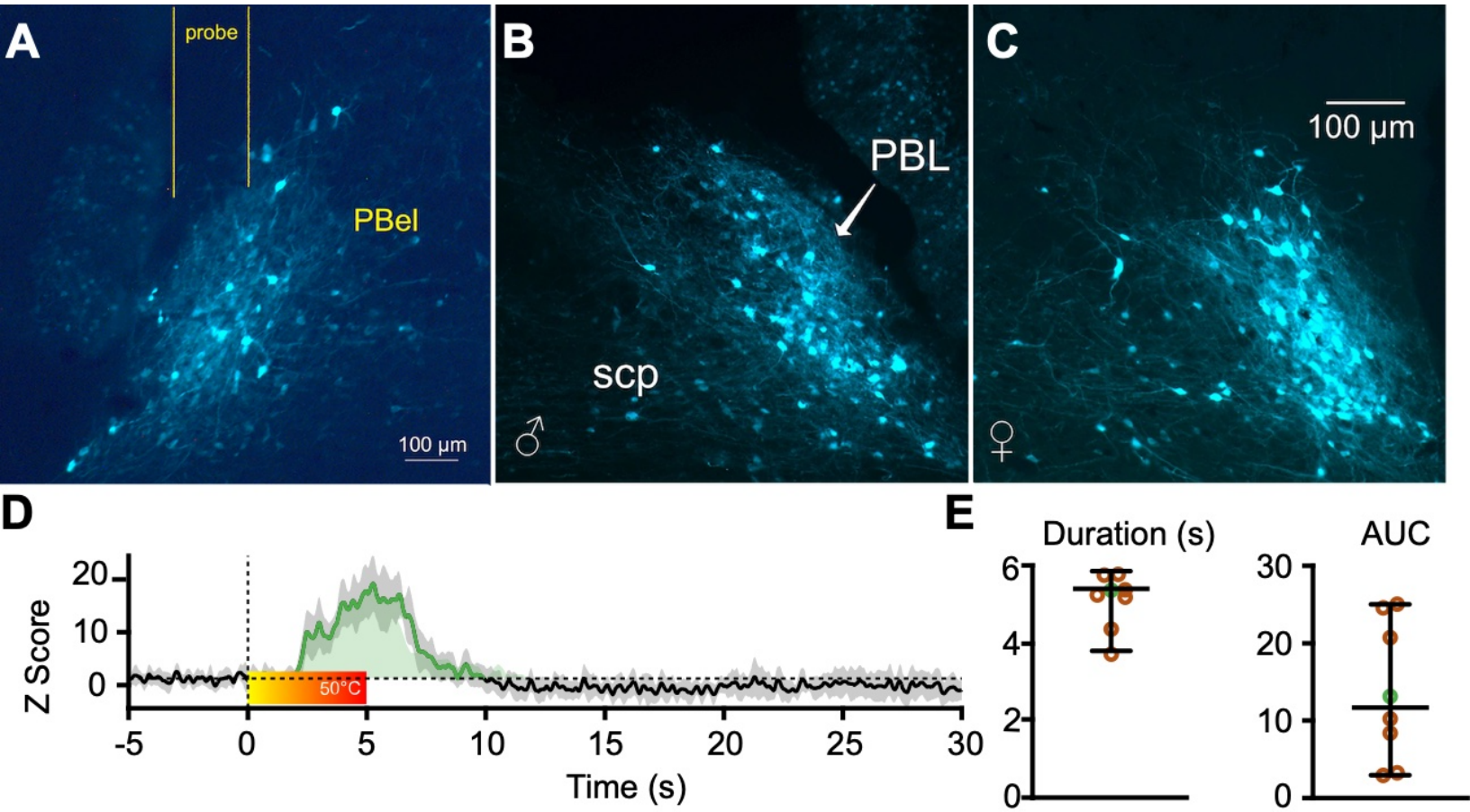
A
probe
PBel
100 µm
B
PBL
scp
♂
C
100 µm
♀
D
Z Score
20
10
0
50°C
-5
0
5
10
15
20
25
30
Time (s)
E
Duration (s)
6
4
2
0
AUC
30
20
10
0

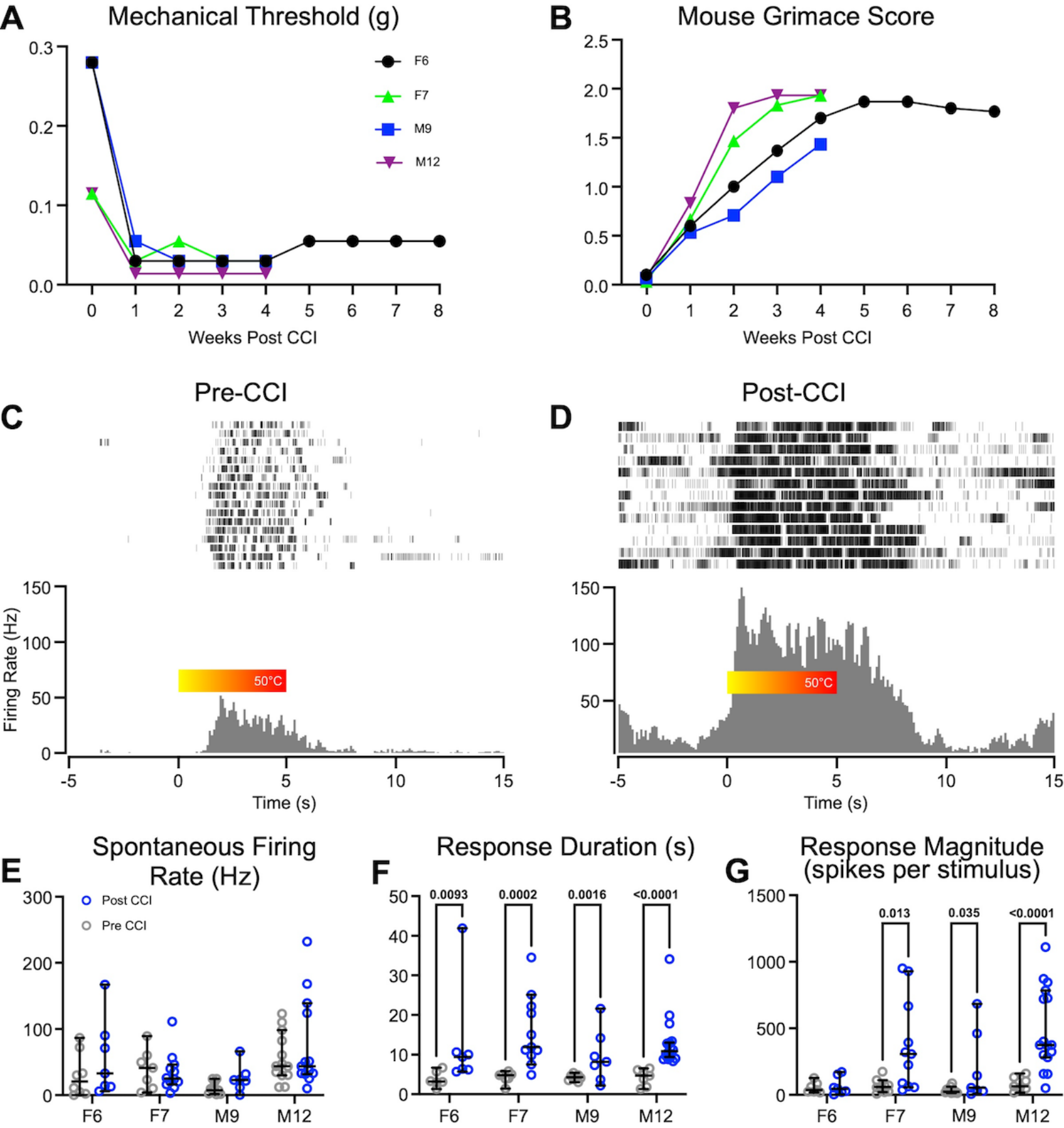
A
Mechanical Threshold (g)
F6
F7
M9
M12
Weeks Post CCI
B
Mouse Grimace Score
Weeks Post CCI
C
Pre-CCI
Firing Rate (Hz)
50°C
Time (s)
D
Post-CCI
50°C
Time (s)
E
Spontaneous Firing Rate (Hz)
Post CCI
Pre CCI
F6
F7
M9
M12
F
Response Duration (s)
0.0093
0.0002
0.0016
<0.0001
G
Response Magnitude (spikes per stimulus)
0.013
0.035
<0.0001

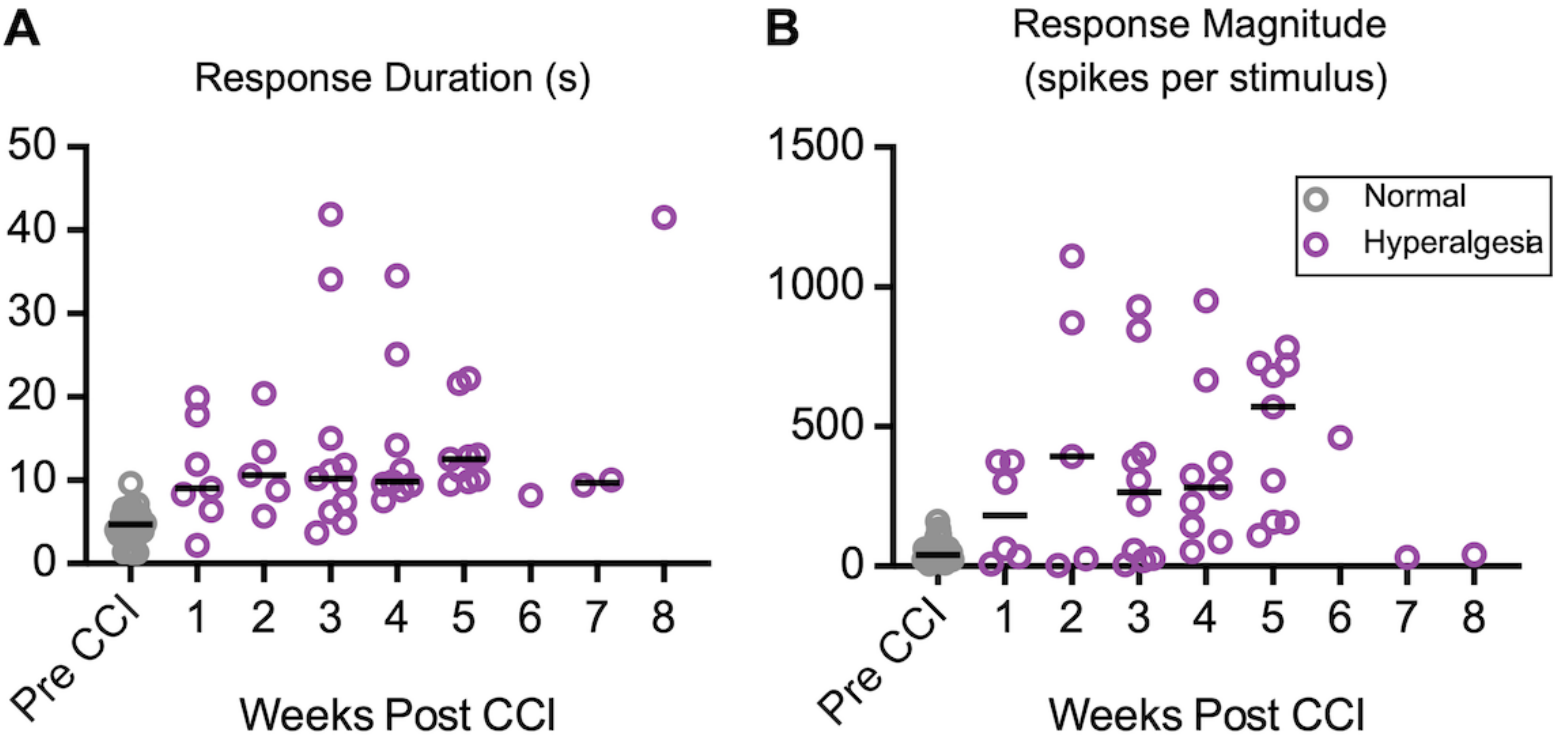
A
Response Duration (s)
50
40
30
20
10
0
Pre CCI
1
2
3
4
5
6
7
8
Weeks Post CCI
B
Response Magnitude
(spikes per stimulus)
1500
1000
500
0
Normal
Hyperalgesia
Pre CCI
1
2
3
4
5
6
7
8
Weeks Post CCI

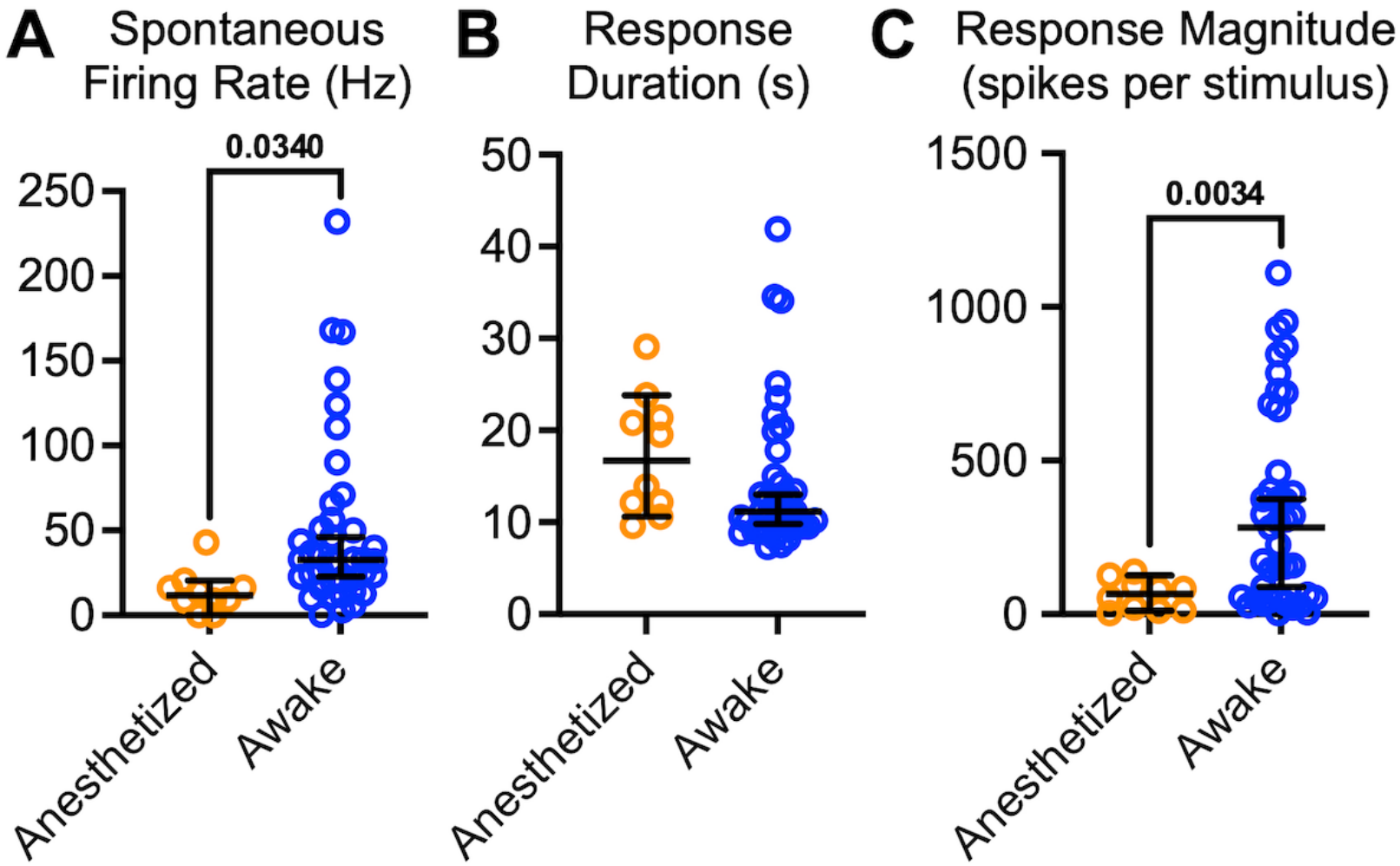
A
Spontaneous Firing Rate (Hz)
0.0340
250
200
150
100
50
0
Anesthetized
Awake
B
Response Duration (s)
50
40
30
20
10
0
Anesthetized
Awake
C
Response Magnitude (spikes per stimulus)
0.0034
1500
1000
500
0
Anesthetized
Awake

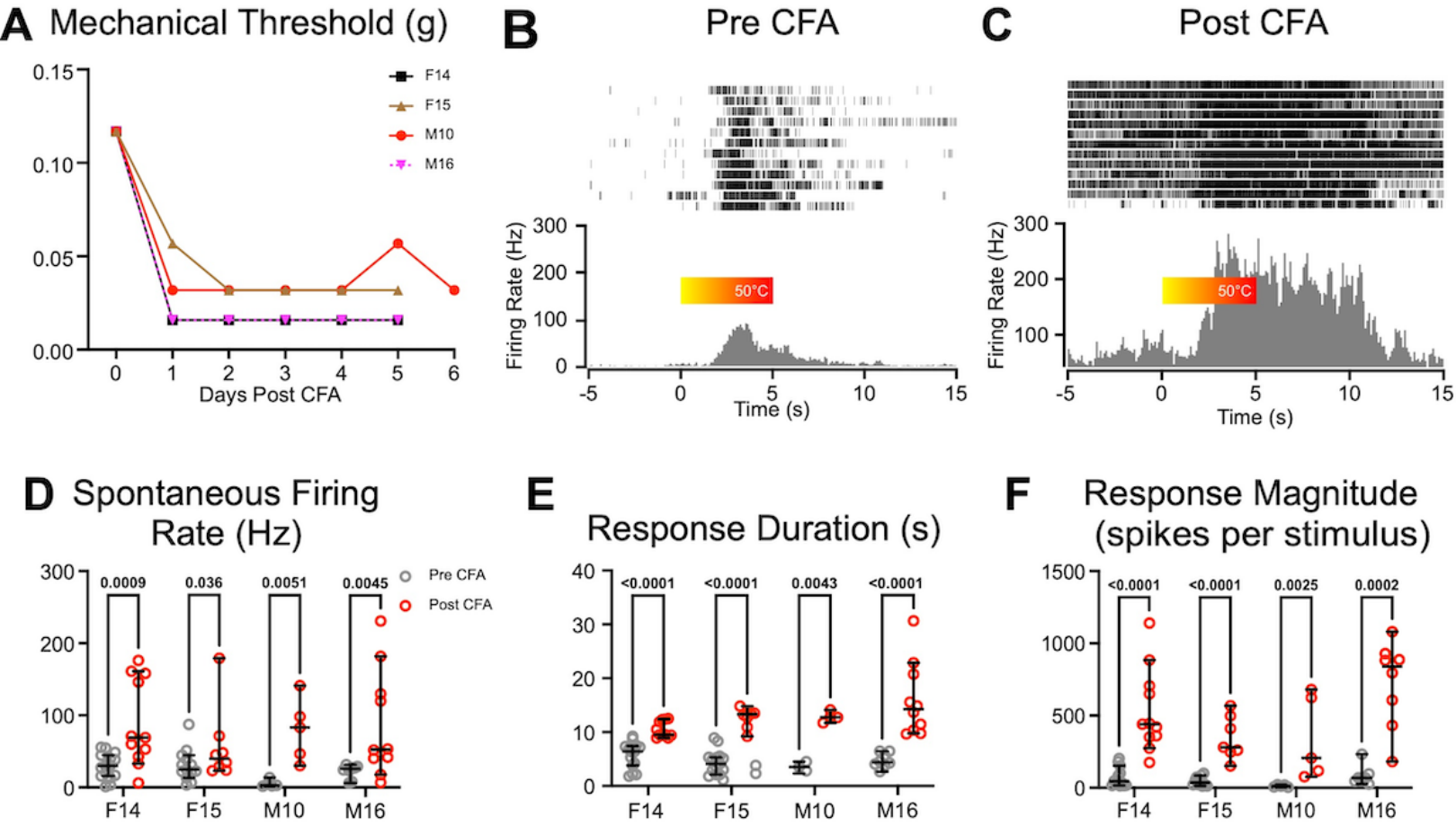
A
Mechanical Threshold (g)
0.15
0.10
0.05
0.00
F14
F15
M10
M16
0
1
2
3
4
5
6
Days Post CFA
B
Pre CFA
Firing Rate (Hz)
300
200
100
0
50°C
-5
0
5
10
15
Time (s)
C
Post CFA
Firing Rate (Hz)
300
200
100
50°C
-5
0
5
10
15
Time (s)
D
Spontaneous Firing Rate (Hz)
300
200
100
0
0.0009
0.036
0.0051
0.0045
Pre CFA
Post CFA
F14
F15
M10
M16
E
Response Duration (s)
40
30
20
10
0
<0.0001
<0.0001
0.0043
<0.0001
F14
F15
M10
M16
F
Response Magnitude (spikes per stimulus)
1500
1000
500
0
<0.0001
<0.0001
0.0025
0.0002
F14
F15
M10
M16

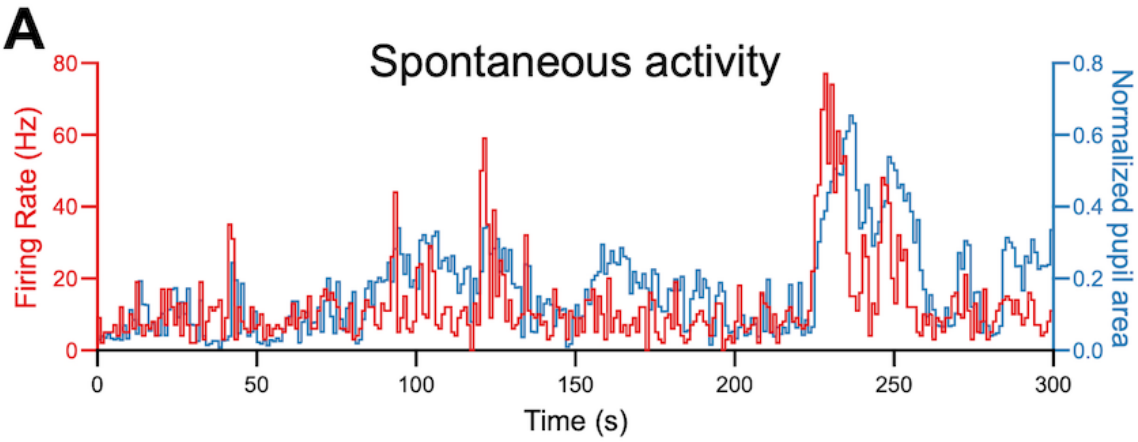
A
Spontaneous activity
Firing Rate (Hz)
Normalized pupil area
Time (s)
0
50
100
150
200
250
300
0
20
40
60
80
0.0
0.2
0.4
0.6
0.8

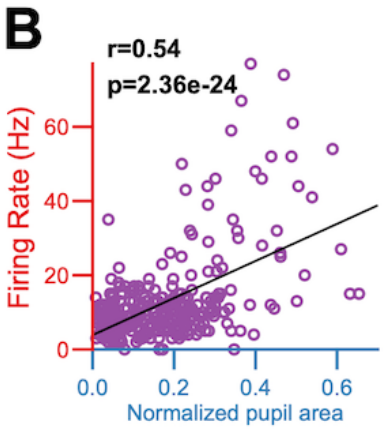
B
r=0.54
p=2.36e-24
Firing Rate (Hz)
Normalized pupil area
0
20
40
60
0.0
0.2
0.4
0.6

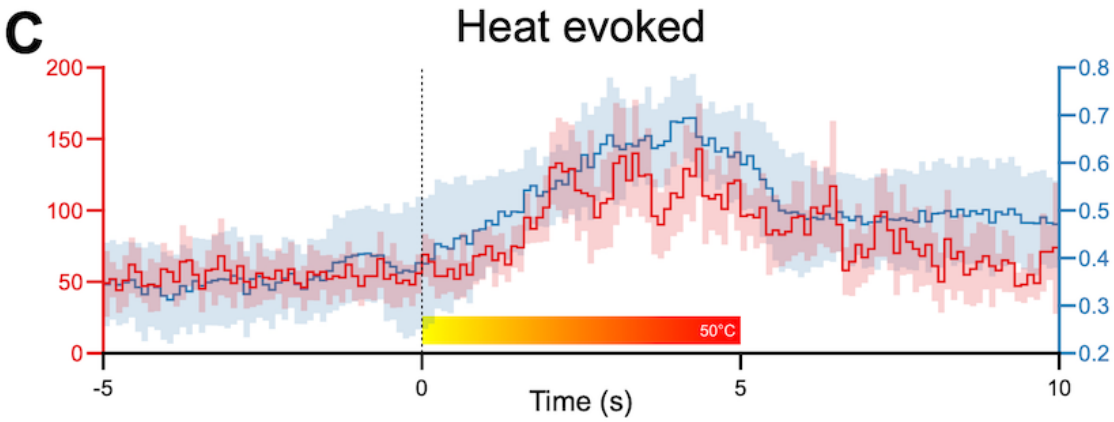
C
Heat evoked
50°C
Time (s)
-5
0
5
10
0
50
100
150
200
0.2
0.3
0.4
0.5
0.6
0.7
0.8

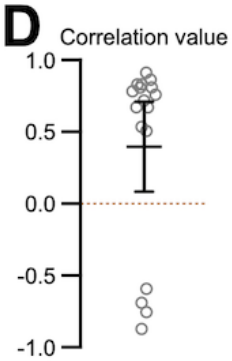
D
Correlation value
1.0
0.5
0.0
-0.5
-1.0

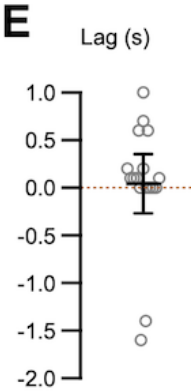
E
Lag (s)
1.0
0.5
0.0
-0.5
-1.0
-1.5
-2.0

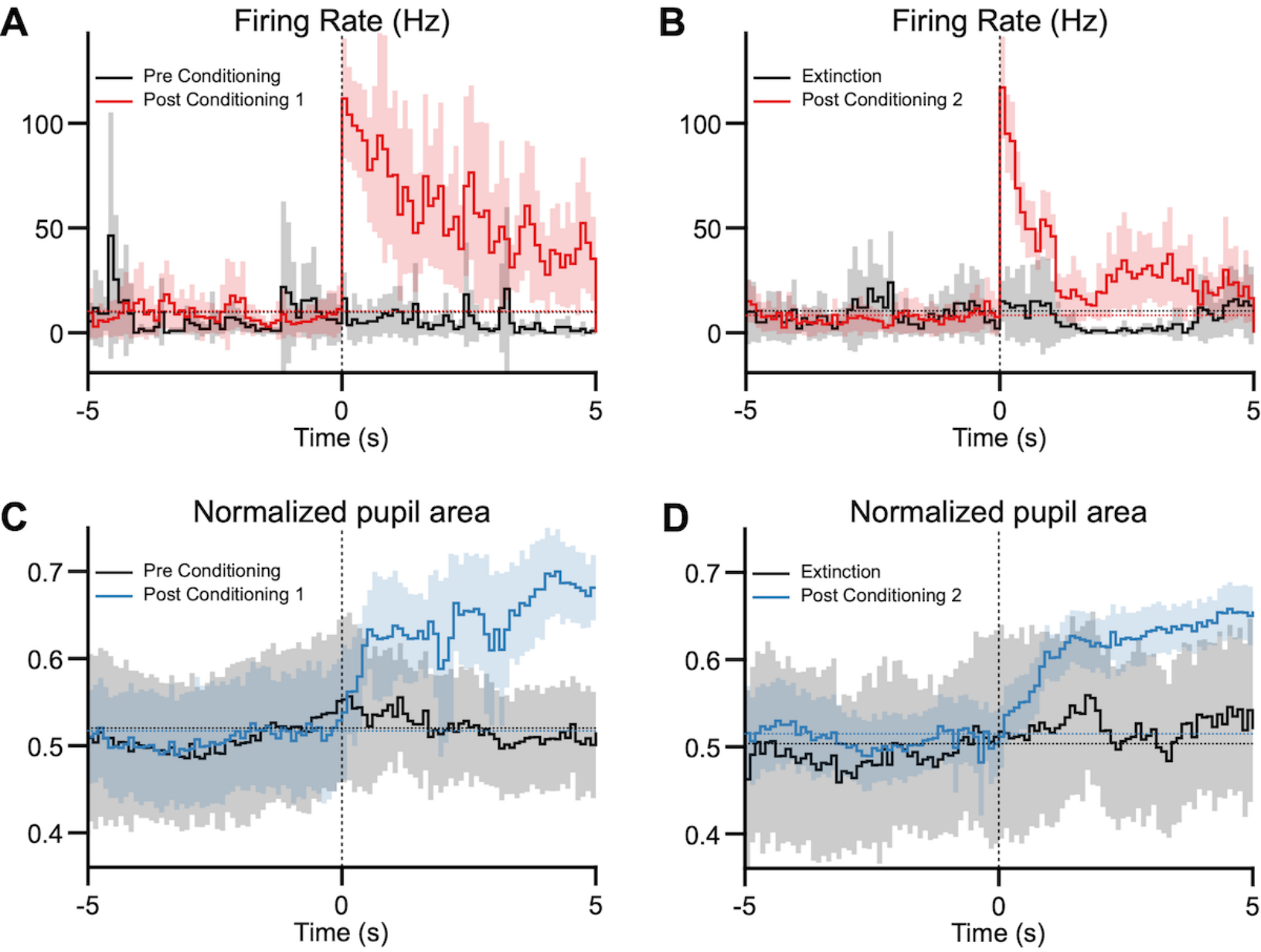
A
Firing Rate (Hz)
Pre Conditioning
Post Conditioning 1
100
50
0
-5
0
5
Time (s)
B
Firing Rate (Hz)
Extinction
Post Conditioning 2
100
50
0
-5
0
5
Time (s)
C
Normalized pupil area
Pre Conditioning
Post Conditioning 1
0.7
0.6
0.5
0.4
-5
0
5
Time (s)
D
Normalized pupil area
Extinction
Post Conditioning 2
0.7
0.6
0.5
0.4
-5
0
5
Time (s)